Measurement of Growth Rate to Determine Condensation Coefficients for Water Drops Grown on Natural Cloud Nuclei

A. M. SINNARWALLA,[1] D. J. ALOFS[1] AND J. C. CARSTENS[2]

Graduate Center for Cloud Physics Research, University of Missouri, Rolla 65401

(Manuscript received 1 July 1974, in revised form 3 September 1974)

ABSTRACT

Growth rate measurements were made for water drops grown on nuclei in atmospheric air samples taken in Rolla, Missouri. Rolla, having a population of 15,000 and very little industry, is relatively free of urban pollutants. The measurements were made in a vertical flow thermal diffusion chamber at supersaturations of 0.5 and 1%. The time to grow from near dry radius to the final radius (6 to 7.5 μm) was measured. If one assumes the thermal accommodation coefficient is unity, the measurements indicate an average value of 0.026 for the condensation coefficient. The temperature ranged from 22.5 to 25.7°C.

1. Introduction

Current meteorological theory (Fukuta and Walter, 1970; Carstens *et al.*, 1974) for the diffusional growth of small water drops takes into account the condensation coefficient β of water vapor molecules impinging on liquid water, and the thermal accommodation coefficient α of air on liquid water. When either α or β becomes $\ll 1$, the growth rate of small drops decreases strongly. According to the theory, α and β influence drop growth through a single parameter (Carstens *et al.*). Therefore, measurements of droplet growth allow one to determine β only if one assumes a value for α, or vice versa. Although α has been measured for water on water (Alty and Mackay, 1935), it appears never to have been measured for air on water.

Mills and Seban (1967) reviewed the experimentally determined values of β for water on water. These values range between 0.006 and 0.42. Mills and Seban feel that the low values are due either to inaccurate surface temperature measurements, contamination of the water surface, or failure to take into account the inadvertent presence of non-condensable gases. In contrast, Delaney *et al.* (1964) and Jamieson (1965) suggest that the polar nature of the water molecule might be expected to result in low values of β for physical situations in which the liquid surface is relatively quiescent. Jamieson reported a time dependence of β, with initial values near unity and rapid relaxation to lower values. This dependence upon exposure time is also supported by recent data by Tamir and Hasson (1971), who report a high value of $\beta(\sim 0.2)$ for short exposure times (2×10^{-3} s).

In view of the above investigations, it appears that our present state of knowledge does not allow an experimental value of β to be extrapolated to a vastly different physical situation. This then suggests that droplet growth calculations should be based upon values of β obtained from droplet growth measurements. For application to atmospheric sciences it is desirable that the drops be grown upon atmospheric cloud nuclei at low supersaturations.

Vietti and Schuster (1973) measured droplet growth rates of airborne water drops grown at relatively high supersaturations in a Wilson chamber on re-evaporation nuclei. The indicated value of β was 0.0065 for $\alpha=1$. However, more recent experiments by Carter and Carstens (1974) with the same apparatus give $\beta=0.023$ for $\alpha=1.0$.

Chodes *et al.* (1974) measured droplet growth rates in a horizontal thermal diffusion chamber. Assuming $\alpha=1$, their average value of β was 0.033, with a standard deviation of 0.005. Essentially, the time to grow from approximately 1.7 μm radius to 2.5 μm radius was measured. They studied 10 drops at each of four different supersaturations (0.40, 0.49, 0.62, 0.72%). Their nuclei were from atmospheric air taken in Jerusalem.

The present paper reports growth rate measurements for water drops grown on nuclei in atmospheric air samples taken in Rolla, Missouri. This city, having a population of 15,000 and very little industry, is relatively free of urban pollutants. The measurements are made in a recently developed (Sinnarwalla and Alofs, 1973) vertical flow thermal diffusion chamber which provides relatively long growth times. The time to grow from near dry radius to the final size of the droplets (6 to 7.5 μm radius) was measured.

2. Description of the chamber

The chamber has been described and analyzed elsewhere (Sinnarwalla and Alofs, 1973; Mahata *et al.*,

[1] Also Department of Mechanical Engineering.
[2] Also Physics Department.

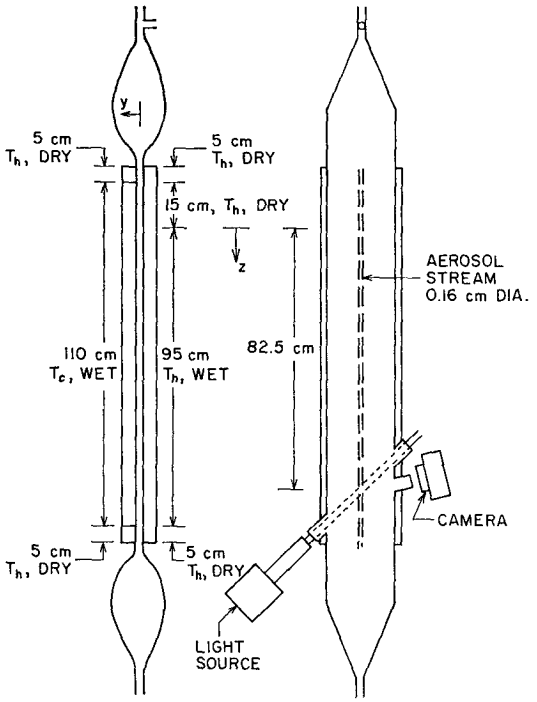

FIG. 1. Schematic of the steady flow vertical plate thermal diffusion chamber.

1973), but subsequent improvements and alterations for the present application require that the chamber be again described.

The 120 cm long by 15 cm wide chamber features steady, laminar flow of air downward between two vertical plates, with a plate spacing d of 1 cm (Fig. 1). The cold plate side of the chamber has a 110 cm long section at the cold plate temperature T_c. The 5 cm long sections at the top and bottom arose due to construction details required to produce a leak-free chamber. The hot plate side of the chamber is kept at the hot plate temperature T_h. For the entire length of the cold plate, and for the central 95 cm length of the hot plate, the inside plate surfaces are covered with filter paper which is continually supplied with distilled water. The upper 20 cm length of the hot plate, however, is dry to avoid transient supersaturations.

As the air flows through the chamber, the local temperature T and water vapor pressure p eventually become linearly proportional to the distance from the cold plate. This produces the same approximately parabolic supersaturation profile which occurs in the conventional static, or zero flow, thermal diffusion chamber. Thus, the supersaturation is a maximum approximately midway between the plates, and drops off rapidly on approach to either plate.

As shown by Sinnarwalla and Alofs the velocity profile in the chamber is given by

$$V=[1-(2y/d)^2][V_c+C(2y/d)], \qquad (1)$$

where V is the local air velocity, positive downward, y the position measured from the midplane between the plates, positive toward the cold plate, d the spacing between the plates, and V_c the centerline velocity, i.e., V at $y=0$. The quantity C is defined as

$$C=\rho B g d^2(T_h-T_c)/(48\,\mu), \qquad (2)$$

where ρ is the average fluid density, B the coefficient of thermal volume expansion, g the gravitational acceleration, and μ the fluid viscosity.

The velocity profiles given by (1) are plotted in Fig. 2 for $T_h=25°C$, $T_c=20°C$, and various values of V_c. It can be seen that for sufficiently small values of V_c, a backflow develops near the hot plate. This backflow is undesirable for reasons described by Sinnarwalla and Alofs. To avoid the backflow, V_c is therefore always kept larger than the following value, obtained from a suitable evaluation of (1):

$$V_c=C\approx 0.43(T_h-T_c). \qquad (3)$$

The supersaturation histories of nuclei passing through the chamber have been investigated in detail (Mahata *et al.*, 1973). These supersaturation histories can be characterized by a supersaturation rise time followed by a steady-state supersaturation S_M.

The maximum available growth time t_A, as limited by phoretic forces, has been given approximately by

$$t_A\approx 35 S_M^{-\frac{1}{2}}. \qquad (4)$$

Moreover the chamber length is such that the limitation on available growth time due to convection effects [Eq. (3)] is also approximately given by Eq. (4).

A schematic of the full system of filtered air flow and aerosol flow is shown in Fig. 3. Most of the air flowing through the chamber is filtered air. The aerosol sample enters the chamber through a 60 cm long inlet tube at the top of the chamber, and flows in a narrow stream (~0.16 cm diameter) down the center of the chamber. The chamber pressure is slightly below (~0.2 cm of water) atmospheric pressure so that the sample is sucked into the chamber. The pressure drop across the sample inlet tube has been calibrated so that the sample flow rate is known by the reading of a pressure trans-

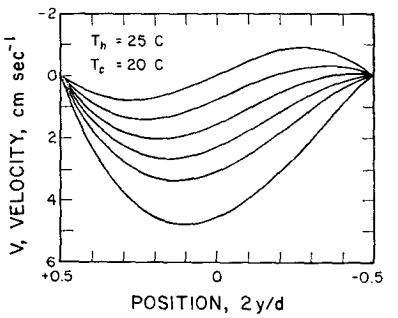

FIG. 2. Velocity profiles obtained from Eq. (1) for $T_h=25°C$, $T_c=20°C$.

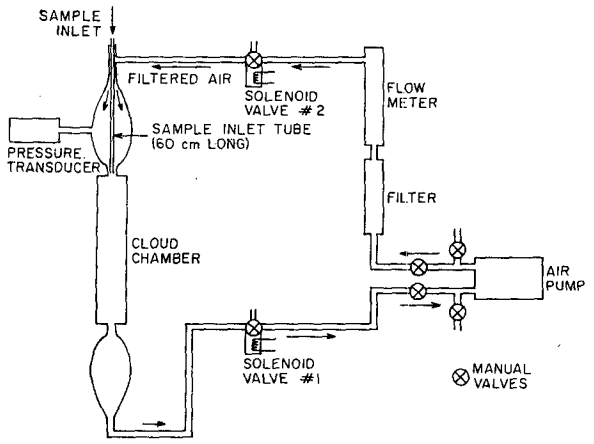

FIG. 3. Schematic of air flow system.

ducer (Fig. 3). The chamber pressure and the filtered air flow rates are controlled by four manual valves attached to the air pump. The filtered air flow rate is measured with a flow meter of the type wherein a ball is suspended by the upflow in a cone-shaped vertical tube.

After the chamber has been operating in steady flow for several minutes, both solenoid valves are simultaneously closed, causing the mass flow rate through the chamber to go to zero within a few hundredths of a second. The terminal velocity of the centerline water drops is then quickly measured by streak photography. More details of this drop sizing technique are given in the next section.

3. Method of sizing the drops

The terminal gravitational settling velocity V_s (cm s^{-1}) of small ($r<10$ μm) water drops falling in air follows Stokes law, which at 25°C is given by

$$V_s=0.0118r^2, \tag{5}$$

where r is the droplet radius (μm). The relaxation time for a 10 μm radius water drop to reach this terminal velocity is 1.23×10^{-3} s (Fuchs, 1964, Table 13), which is negligibly small in the present application. Stokes law then constitutes the basis for measuring the size of drops produced in the chamber. The sequence of events is as follows:

Immediately after the solenoid valves are closed, pressure waves travel at the speed of sound through the rectangular channel formed by the hot and cold plates. These pressure waves reflect from the inlet and outlet ducts, which serve as plenum chambers at each end of the channel. To estimate roughly the efficiency of each reflection from a plenum chamber, we approximate these ducts as sudden expansions. The following formula for the reflection efficiency R is given by Davies (1957):

$$R=(m-1)/(m+1), \tag{6}$$

where m is the areal expansion ratio, and R the ratio of the sound pressure of the reflected wave to that of the incident wave. This ratio is the same as the ratio of the velocity jumps across the reflected and incident waves. In the present case, the reflection efficiency is indicated to be 88%. Within a time interval of 0.2 s, about 50 reflections have occurred, and the wave amplitude has decayed to $(0.88)^{50}$, or about 0.3% of the original amplitude. For the present purpose, this residue is sufficiently small to be neglected.

To verify the above result, the following separate experiment was performed. With both plates dry and at the same temperature, an aerosol of 1 μm radius polystyrene latex spheres was passed through the chamber with various air velocities. After operating the chamber in steady flow, the solenoid valves were suddenly closed, and the movement of these particles was observed. Since these particles have a Stokes velocity near 0.012 cm s^{-1}, they should appear to be virtually stationary within 0.2 s after shutting the solenoid valves. Such was indeed found to be the case. Moreover, in the subsequent 1.0 s time interval, the particles were observed to be falling near their Stokes velocity. This experiment also indicates that the mercury vapor light source used for illumination does not cause a significant convection current by heating the air.

For practical purposes, then, the velocity profile in the chamber is described by (1), with a zero value of V_c after shutting the valves. Thus the velocity profile has the shape of the top curve in Fig. 2. It can be seen that the air velocity becomes positive or negative as one moves away from the mid-plane ($y=0$), and therefore only the water drops very near $y=0$ move at their Stokes velocities.

About 0.5 s after the solenoid valves are shut, the shutter on the camera is opened and a streak photograph of the droplets is taken. Each photograph shows the two sidewalls of the chamber, as well as the droplet streaks. After the film is developed, it is projected in a film reader which has been calibrated so that the streak length can be measured. In reading the film, only the streaks located within $y=\pm\epsilon$ are used as data. The slope of velocity profile at $y=0$, as obtained from (1) and (2), is

$$dv/dy=2C. \tag{7}$$

In the present investigation, the maximum available growth time was always used, so that (3) applies. Thus,

$$dv/dy=2V_c, \tag{8}$$

where V_c is the centerline velocity before the solenoid valves are shut.

The air velocity at $y=\pm\epsilon$ is then

$$dv=\pm2V_c\epsilon. \tag{9}$$

In the present investigation $\epsilon=0.025$ cm, so that

$$dv=\pm0.05V_c. \tag{10}$$

Applying (10) to the data presented in Section 5 results in respective error limits of ±15 and ±17% on the measured Stokes velocity at $S=1$ and 0.5%. The corresponding error limits on drop radius are ±7.5 and ±8.5%.

4. Growth calculations

Growth calculations were made by using the analysis given by Carstens *et al.* (1974) for solution drops. Values used for various transport coefficients and other quantities are listed in Table 1. Throughout the calculations, the thermal accommodation coefficient was taken as unity. The nuclei were assumed to be NaCl with no insoluble fraction, but this assumption only weakly influences the growth behavior in the size where Raoult's law is valid. This is so, because the effects of chemical composition and solubility fraction can be included in one fundamental nucleus parameter, either the critical supersaturation S_c of the nucleus, or the equilibrium radius of the nucleus at 100% humidity (Berry, 1966; Alofs and Podzimek, 1974).

The supersaturation histories used in the growth equation are defined by Eqs. (6) and (9) in the paper by Mahata *et al.* (1973). Fig. 4 shows the supersaturation histories for data runs 1 and 3. The time begins when a nucleus passes $z=0$ (Fig. 1). At this instant the humidity is less than 100%. The supersaturation then rises almost exponentially with time, from that value to its final value. The time for supersaturation to rise to 90% of its final value varies from 2.32 to 2.66 s for the conditions of the present investigation.

The growth calculations showed that the rate of supersaturation rise is sufficiently slow, so that as the humidity reaches 100%, the drops are at very nearly their equilibrium radii, as long as the nuclei have $S_c>0.1\%$. Because of this fact, the effect of deviations from Raoult's law (Low, 1969) at smaller drop sizes does not affect the growth calculation as the drops become larger.

TABLE 1. Thermophysical properties used (notation from Carstens *et al.*, 1974).

	Temperature (°C)			
	21	23	25	27
D ($cm^2\ s^{-1}$)	0.2455	0.2485	0.2514	0.2544
K (10^{-4} cal $cm^{-1}\ °C^{-1}$)	0.6077	0.6110	0.6144	0.6177
L (10^{-4} cal g^{-1})	0.2125	0.2145	0.2164	0.2183
ρ_{eq} (10^{-4} g cm^{-3})	0.1834	0.2058	0.2306	0.2579
b (10^{-} g $cm^{-3}\ °C^{-1}$)	0.1066	0.1178	0.1390	0.1430

Fig. 5 shows the final radius indicated by the theoretical calculations for runs 1 and 3. The ordinate shows values of β, and the abscissa the drop radius at $z=82.5$ cm. It should be pointed out that because of gravitational fall, the large drops resulting from larger β experience a shorter growth time in traveling the 82.5 cm distance from $z=0$ to the station where the drops are sized (Fig. 1).

The solid curves in Fig. 5 are for a nucleus with critical supersaturation S_c of 0.35% and the dotted curves for a nucleus with $S_c=0.035\%$. Since for a typical nucleus spectrum there will be many more nuclei with $S_c<0.35\%$ than with $S_c<0.035\%$, the solid curves are used in correlating the data to obtain β. The error analysis of Section 6 shows that other experimental uncertainties give a cumulative error limit of −12.5 to +9.5% on final drop radius. In view of these other uncertainties, the effect of nucleus size seen in Fig. 5 is small.

5. Results

The experimental results are shown in Figs. 6–9. Each data set took about ~3 h to run, on the day whose date is indicated. In all cases except Fig. 9, the sample

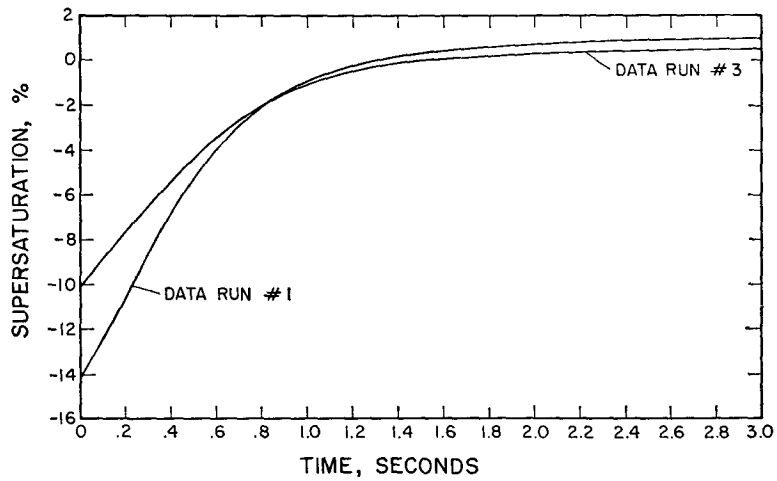

FIG. 4. Supersaturation histories for data runs 1 and 3.

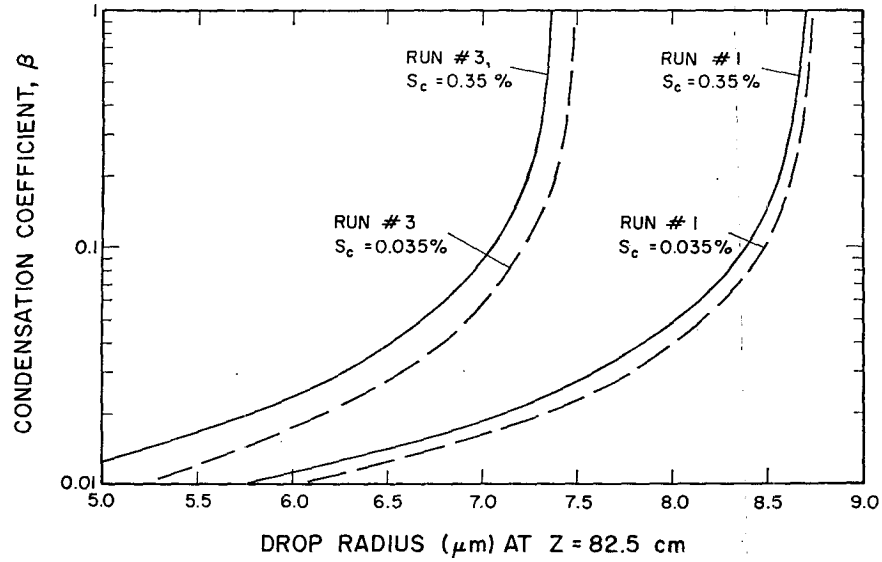

FIG. 5. Theoretical calculations for run 1 and 3 showing radius at $z=82.5$ cm vs β.

air was taken from immediately outside the laboratory building in Rolla. For the data of Fig. 9, the air sample was room air.

The ordinate in each figure is the number of drops observed in the intervals of terminal velocity shown on the abscissa. The lower abscissas show the corresponding value of drop radius and condensation coefficient. The circle on each figure shows the average value of terminal velocity $\bar{V}_s$. The value of drop radius obtained from Stokes law for $\bar{V}_s$ is called the average drop radius $\bar{r}$. The error flags in Figs. 6–9 show the error limits as obtained from the error analysis, in the next section. The value of β corresponding to $\bar{V}_s$, or $\bar{r}$, is called the average β, and this value is also indicated on each figure.

Figs. 6 and 7 are for approximately $S=1\%$ and indicate average β values of 0.032 and 0.021, respectively. The lower average value of β from Fig. 7 is accompanied

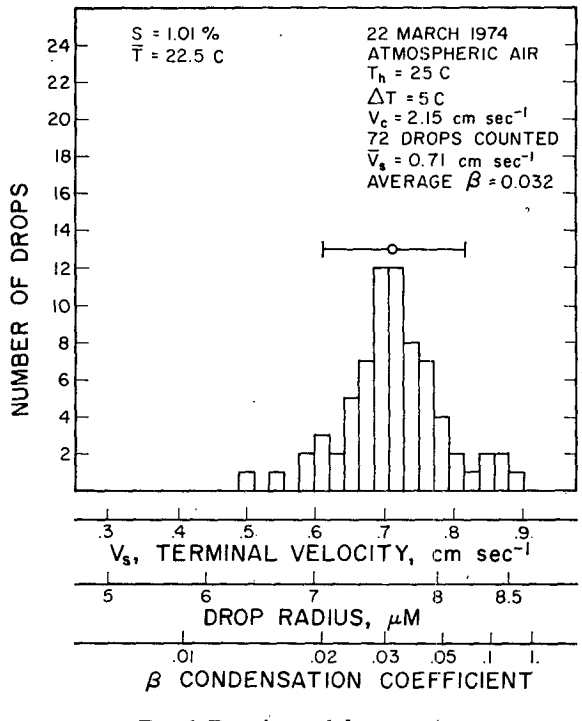

FIG. 6. Experimental data, run 1.

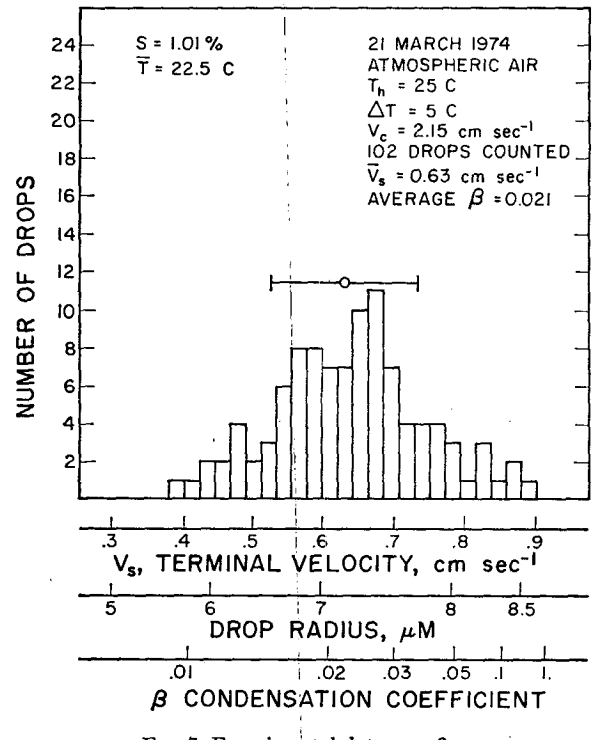

FIG. 7. Experimental data, run 2.

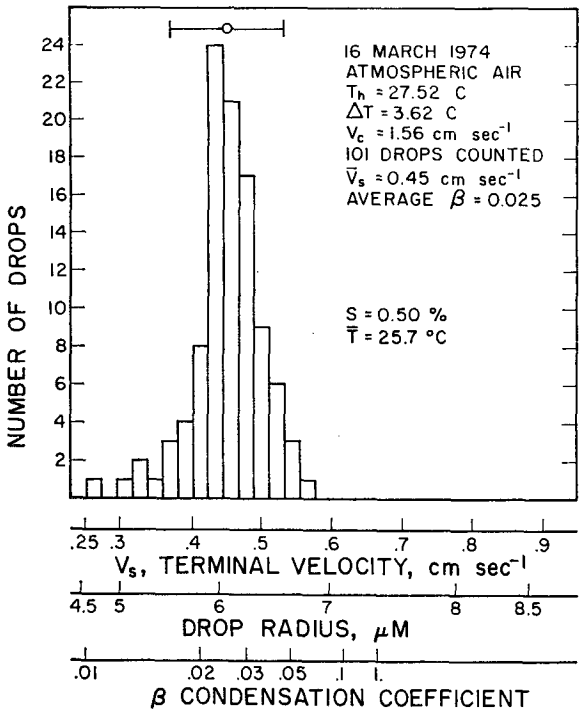

FIG. 8. Experimental data, run 3.

by a higher spread in drop sizes. This behavior is possibly due to variations in atmospheric contaminants on the day the data were taken.

Figs. 8 and 9 are approximately $S = 0.5\%$ and indicate average β values of 0.025 and 0.029, respectively. These values are nearly the same as for $S = 1.0\%$, which lends some confidence in the theory and in the experiment.

As to the spread in the observed values of β, it can be seen from Figs. 6–9 that not all the observed spread is likely to be due to the error limits of the experiments. Thus, there is an indication that not all the drops had the same value of β. The standard deviation of the indicated values of β is below 0.01 for all the data runs.

If one averages the values of average β given in Figs. 6–9, with a weighting factor for each data run proportional to the number of drops in the data run, then the overall average β is found to be 0.026. This value is in relatively good agreement with the value of 0.022 obtained by Carter and Carstens (1974) and the value of 0.033 reported by Chodes *et al.* (1974). In view of the fact that the drops studied by Carter and Carstens were initially formed by homogeneous nucleation, the above good agreement indicates that the cloud nuclei in our experiment and in that of Chodes *et al.* did not reduce β by providing surface contaminants. This does not rule out the possibility that contamination by adsorption during drop growth influenced all three investigations. Nor does it rule out the possibility that some cloud nuclei, perhaps those near cities, might further reduce β by providing contamination.

6. Error analysis

Five possible sources of error are discussed in this section.

1) To calibrate the flowmeter, it was connected in series with a 50 cm^3 burette showing 1 cm^3 divisions. Movement of air through the burette was monitored by the movement of a thin film of soap solution which traversed the burette cross section, and the time required for 50 cm^3 of air to flow through the burette was measured. After this calibration, the accuracy of the flowmeter is estimated to be $\pm 2\%$. This uncertainty influences calculated growth time so as to cause an equivalent uncertainty of $\pm 1\%$ in drop radius.

2) The camera shutter was always set at 0.5 s. To determine the time for which the shutter actually remained open, the shutter was placed between a light source and a photomultiplier (PM) tube. The output of the PM tube was amplified and recorded on an oscillograph recorder. The recorder had a frequency response of 1000 Hz, whereas the PM tube and the amplifier had much faster responses.

The results showed that for the half-second shutter setting, the shutter took 0.003 s to fully open, remained fully open for 0.454 s, and took another 0.003 s to close. Thus the time during which the shutter was at least 50% open was 0.457 s, which was the time used in correlating the data. This behavior of the shutter was found to be very reproducible. The uncertainty is therefore only ± 0.003 s out of 0.457 s. This uncertainty

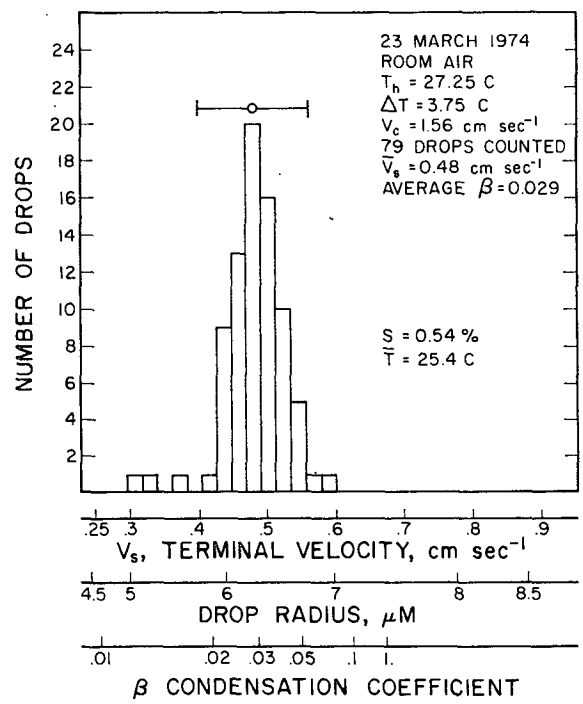

FIG. 9. Experimental data, run 4.

is equivalent to $\pm 0.3\%$ uncertainty in measured drop radius.

3) Any error in the measurement of temperature difference between the two plates results in an error in the calculated supersaturation. Ten copper-constantan thermocouples installed at various locations in the two plates indicated that both plate surfaces were isothermal to within ± 0.05°C. The thermocouples were calibrated against a quartz thermometer. This calibration indicated that the measurement of $(T_h - T_s)$ is within $\pm 3.5\%$ of its actual value, and the measurement T_h is within ± 1°C of its actual value. By use of the computer program for drop growth rate, these uncertainties in temperature measurement were found to give rise to a $\pm 4\%$ uncertainty in drop radius.

4) The effect of vapor depletion and condensation heat release by the growing drops constitutes another source of error. Hudson and Squires (1973) have analyzed this effect for a horizontal thermal diffusion chamber featuring steady flow, in which filtered air surrounds the aerosol; the aerosol was contained in a sheet 8 cm wide by 0.2 cm thick, located midway between the two plates. Their expression for the reduction in supersaturation S_R is

$$S_R = 2.5 \times 10^{-4} S \sigma r d, \tag{11}$$

where S_R and S are in percent, σ (cm^{-2}) is the areal number density of drops, r (μm) the radius of the drops, and d (cm) the spacing between the plates.

For the present vertical chamber, σ is given by

$$\sigma = n/bh, \tag{12}$$

where b is the diameter of the aerosol stream outside of which there are no droplets, h a specified length of this stream, and n the number of droplets in the volume thus defined. In the present experiments, b was 0.16 cm and h was taken to be the vertical height (0.7 cm) of the illumination light beam. The horizontal width of this light beam was 0.1 cm; hence, if n_0 is the number of droplets observed in the light beam, the value of n for Eq. (12) is 1.6 n_0.

Most of the times, 1–3 drops were observed in the illumination beam and recorded on the photographs. Thus, taking an upper limit on n_0 to be 3, an upper limit on n is $n = 4.8$. It should be mentioned here that the nuclei concentration was deliberately reduced by a factor varying from 3 to 50 in order to obtain the above low value of n_0. This reduction in concentration is indicated by calculations of the diffusional losses of nuclei in the sample inlet system, for sample flow rates of 0.03 to 0.09 cm^3 sec^{-1}. With $n = 4.8$, $b = 0.16$ cm and $h = 0.7$ cm, Eq. (12) gives $\sigma = 42.8$ cm^{-2}, and for plate spacing $d = 1$ cm, Eq. (11) then gives

$$S_R = 1.07 \times 10^{-2} S r. \tag{13}$$

Since the data presented in Section 5 show an average r of 6 μm for $S = 0.5\%$, Eq. (13) gives $S_R = 0.065\ S$. At $S = 1\%$, it turns out that $S_R = 0.08\ S$. Thus the maximum effect of vapor depletion and condensation heat release is to reduce the final supersaturation by at most 8% of its nominal value. Separate calculations indicate that this could reduce final drop size by at most 3%.

5) Another error concerns the velocity profile in the chamber during the time the camera shutter is open. This error has been already discussed in Section 3, and found to result in a maximum error limit of $\pm 8.5\%$ on drop radius. This error limit is larger than any of the other possible sources of error discussed above.

Error Accumulation

Except for the effect of vapor depletion, all of the errors described above are random errors. To accumulate the random errors, the method of quadrature, or root mean square is used. The vapor depletion error is then added to this result, and an overall error limit on drop radius is thus found to be -12.5 to 9.5%. The error flags in Figs. 6–9 indicate this error limit as applied to the average drop radius. These error limits on β cover the range 0.015 to 0.07, considering all four data sets. The average β corresponding to the average radius is also given in these figures. The range of these values of β, considering all four data sets, is 0.021 to 0.032.

7. Conclusions

The present investigation, together with that of Chodes *et al.* (1974) and Carter and Carstens (1974), suggests using $\beta = 0.022$–0.032, $\alpha = 1$, as average values in the diffusional growth subroutine of future cloud modeling computations. The above conclusion is preliminary, however, because nuclei taken at different altitudes and geographic locations might differ in their degree of contamination. Also, β may depend on temperature, since the above three investigations cover only the small temperature range of 19 to 27°C.

Acknowledgments. This work was supported by the Atmospheric Sciences Section, National Science Foundation, under Grant GA-30876, and by the Army Research Office. Mr. James Blessing assisted in the computer work.

REFERENCES

Alofs, D. J., and J. Podzimek, 1974: A review of Laktinov's isothermal cloud nucleus counter. *J. Appl. Meteor.*, **13**, 511–512.

Alty, T., and Mackay, 1935: The accommodation coefficient and the evaporation coefficient of water. *Proc. Roy. Soc. London*, **A149**, 104–116.

Berry, E. X, 1966: A convenient nucleus parameter for considerations of droplet growth. *J. Rech. Atmos.*, **2**, 411–416.

Carstens, J. C., J. Podzimek and A. Saad, 1974: On the analysis of the condensational growth of a stationary cloud drop in the viscinity of activation. *J. Atmos. Sci.*, **31**, 592–596.

Carter, J. M., and J. C. Carstens, 1974: Experimental corroboration of conventional meteorological theory of cloud drop growth by laser scattering. *Trans. Amer. Geophys. Union*, **55**, 267–268.

Chodes, N., J. Warner and A. Gagin, 1974: A determination of the condensation coefficient of water from the growth rate of small cloud droplets. *J. Atmos. Sci.*, **31**, 1351–1357.

Davies, D. D., 1957: Acoustical filters and mufflers. *Handbook of Noise Control*, C. M. Harries, Ed., McGraw-Hill, p. 21.

Delaney, L. J., K. W. Houston and L. C. Eagleton, 1964: The rate of vaporization of water and ice. *Chem. Eng. Sci.*, **19**, 105–114.

Fuchs, N. A., 1964: *The Mechanics of Aerosols*. Pergamon Press, 408 pp.

Fukuta, N., and L. A. Walter, 1970: Kinetics of hydrometeor growth from a vapor-spherical model. *J. Atmos. Sci.*, **27**, 1160–1172.

Hudson, J., and P. Squires, 1973: Evaluation of a recording continuous cloud nucleus counter. *J. Appl. Meteor.*, **12**, 175–183.

Jamieson, D. T., 1965: The condensation coefficient of water. *Proc. Third Symp. Thermophysical Properties*, ASME, 230–236.

Low, D. H., 1969: A theoretical study of nineteen condensation nuclei. *J. Rech. Atmos.*, **5**, 65–78.

Mahata, P. C., D. J. Alofs and A. M. Sinnarwalla, 1973: Supersaturation development in a vertical-flow thermal diffusion chamber. *J. Appl. Meteor.*, **12**, 1379–1383.

Mills, A. F., and R. A. Seban, 1967: The condensation coefficient of water *Intern. J. Heat Mass Transfer*, **10**, 1815–1827.

Sinnarwalla, A. M., and D. J. Alofs, 1973: A cloud nucleus counter with long available growth time. *J. Appl. Meteor.*, **12**, 831–835.

Tamir, A., and D. Hasson, 1971: Evaporation and condensation coefficient of water. *Chem. Eng. J.*, **2**, 200–211.

Vietti, M. A., and B. G. Schuster, 1973: Laser scattering measurement of droplet growth in binary mixtures: Part I, H_2O and air. *J. Chem. Phys.*, **58**, 434–441.